

Figure S1. Pedigrees of families 1, 2, and 3.

Circles indicate females; squares, males; and diamonds, unknown sex. Black indicates deceased and white, living. Arrows mark individuals from whom fibroblasts were used for Western blot analysis. An additional child was identified in family 3 heterozygous for the *MPC1* T236A allele. Adapted from (7).

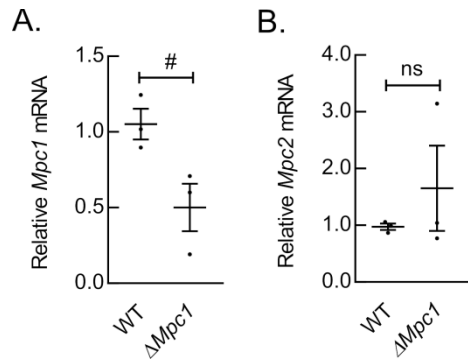


Figure S2. $\Delta Mpc1$ cells show a specific loss of *Mpc1* but not *Mpc2*.

A-B) Quantification of *Mpc1* (A) and *Mpc2* (B) transcript in WT C2C12 (WT) cells and $\Delta Mpc1$ cells (N=3).

Data are presented as mean \pm SEM. Two-tailed unpaired t-test was performed for Figure S2A-S2B (# $p \leq 0.05$, ns= not significant).

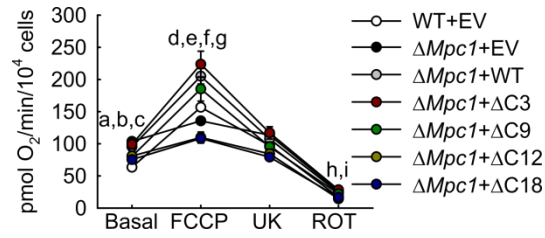


Figure S3. MPC1 C-terminal truncations cause MPC complex instability.

Respiration by driven 10 mM pyruvate in WT C2C12 cells transduced with a vector expressing guideless Cas9 and subsequently with an empty vector (WT+EV) compared $\Delta Mpc1$ cells complemented with an empty vector (EV), WT human MPC1 (WT), or with MPC1 mutants C-terminally truncated by 3 ($\Delta C3$), 9 ($\Delta C9$), 12 ($\Delta C12$), or 18 amino acids ($\Delta C18$). Letters indicate significant difference in basal respiration among $\Delta Mpc1+\Delta EV$, $\Delta Mpc1+WT$, $\Delta Mpc1+\Delta C3$ (a-c; $P \leq 0.001$) versus WT+EV, in FCCP-stimulated respiration among $\Delta Mpc1+\Delta C3$ (d; $P \leq 0.01$); $\Delta Mpc1+WT$, $\Delta Mpc1+\Delta C12$, $\Delta Mpc1+\Delta C18$ (e-g; $P \leq 0.05$) versus WT+EV, and in rotenone-inhibited respiration among $\Delta Mpc1+\Delta C3$ (h; $P \leq 0.01$), $\Delta Mpc1+EV$ (i; $P \leq 0.05$) versus WT+EV (N=9; 3 clone lines/genotype x 3 technical replicates/clone line).

Data are presented as mean \pm SEM. One-way ANOVA was performed for Figure S3.

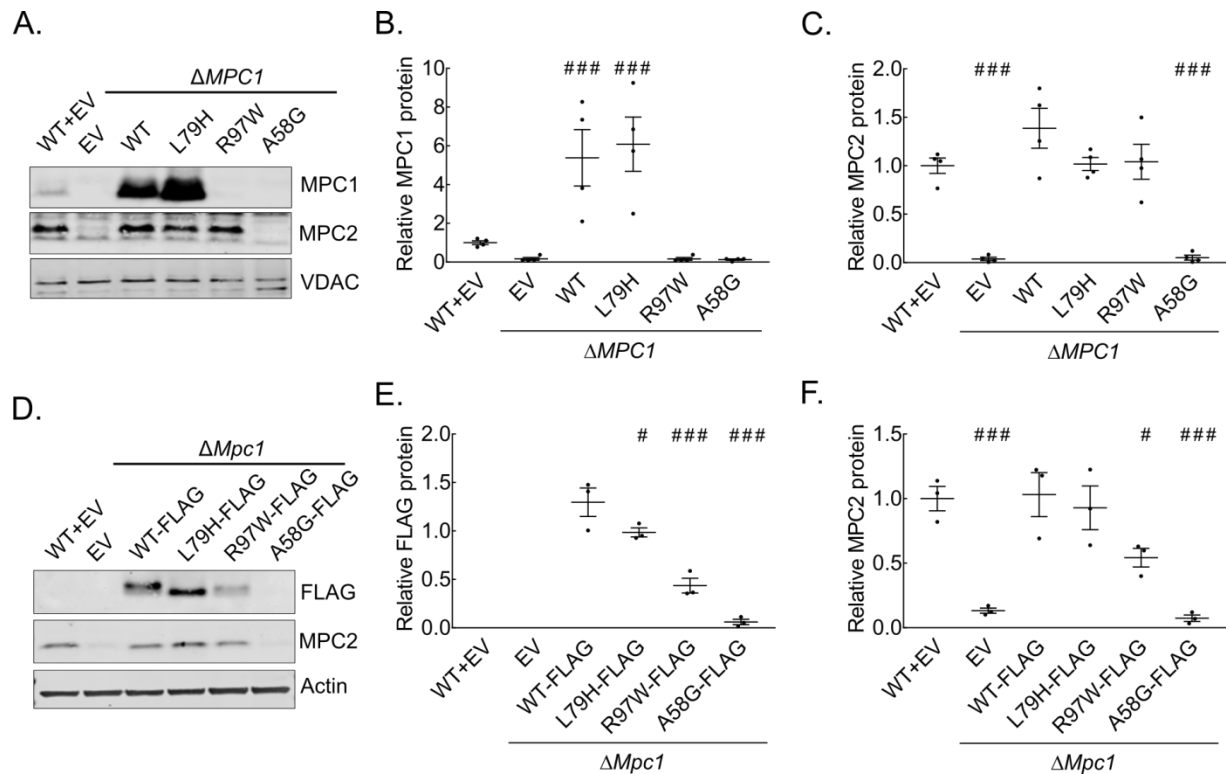


Figure S4. Δ MPC1 complementation by MPC1 WT, mutant L79H, and mutant R97W stabilize MPC2 protein.

A) Representative MPC1, MPC2, and VDAC levels visualized by immunoblot in WT HEK 293T cells transduced with a vector expressing guideless Cas9 and subsequently with empty vector (WT+EV), as compared to Δ MPC1 cells complemented with empty vector (EV), MPC1 (WT), and MPC1 mutants (L79H, R97W, and A58G) (N=4).

B-C) Quantification of relative MPC1 (B) and MPC2 (C) protein levels relative to VDAC as compared to WT+EV (N=4).

D) Representative FLAG, MPC2, and Actin levels visualized by immunoblot in WT C2C12 cells transduced with a vector expressing guideless Cas9 and subsequently with empty vector (WT+EV), compared to Δ Mpc1 cells complemented with empty vector (EV), or C-terminally FLAG-tagged WT human MPC1 (WT-FLAG) and MPC1 mutants (L79H-FLAG, R97W-FLAG, and A58G-FLAG) (N=4)

E-F) Quantification of relative FLAG (E) and MPC2 (F) protein levels relative to VDAC compared to Δ Mpc1+WT-FLAG (E) or WT+EV (F) (N=3).

Data are presented as mean \pm SEM. One-way ANOVA was performed for Figure S4A, S4B, S4E, and S4F (### $p \leq 0.001$).

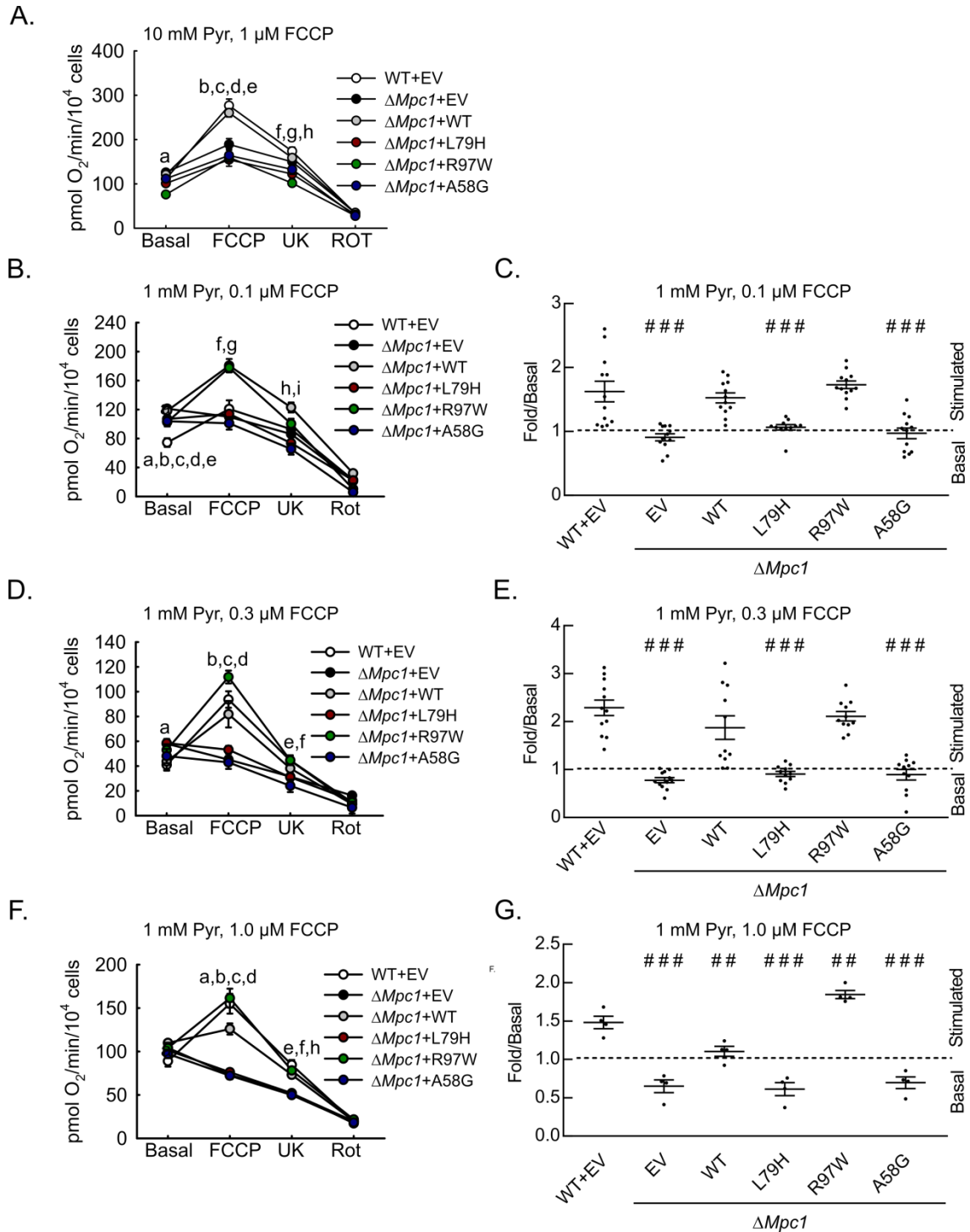


Figure S5. Phenotypic differences of MPC1 mutants is maintained a decreased pyruvate concentration and altered FCCP concentration.

A) Respiration driven by 10 mM pyruvate in WT C2C12 cells transduced with a vector expressing guideless Cas9 and subsequently with an empty vector (WT+EV) compared to Δ Mpc1 cells complemented with an empty vector (EV), plus WT human MPC1 (WT),

or the MPC1 mutants (L79H, R97W, and A58G). Letters indicate significant difference in basal respiration among $\Delta Mpc1+R97W$ (**a**; $P \leq 0.001$) versus WT+EV, in FCCP-stimulated respiration among $\Delta Mpc1+EV$, $\Delta Mpc1+L79H$, $\Delta Mpc1+R97W$, $\Delta Mpc1+A58G$ (**b-e**; $P \leq 0.05$) versus WT+EV, and in UK5099-inhibited respiration among $\Delta Mpc1+L79H$, $\Delta Mpc1+R97W$ (**f-g**; $P \leq 0.001$), $\Delta Mpc1+A58G$ (**h**; $P \leq 0.01$) versus WT+EV (N=12; 2 clone lines/genotype x 6 technical replicates/clone line).

B) Respiration driven by 1.0 mM pyruvate in cells described in **A**). 0.1 μ M FCCP was injected when indicated. Letters indicate significant difference in basal respiration among $\Delta Mpc1+EV$, $\Delta Mpc1+WT$, $\Delta Mpc1+L79H$, $\Delta Mpc1+R97W$, $\Delta Mpc1+A58G$ (**a-e**; $P \leq 0.001$) versus WT+EV, in FCCP-stimulated respiration among $\Delta Mpc1+WT$, $\Delta Mpc1+R97W$ (**f-g**; $P \leq 0.001$) versus WT+EV, and in UK5099-inhibited respiration among $\Delta Mpc1+WT$ (**h**; $P \leq 0.01$), $\Delta Mpc1+A58G$ (**h**; $P \leq 0.05$) versus WT+EV (N=12; 2 clone lines/genotype x 6 technical replicates/clone line).

C) Quantification of FCCP-stimulated normalized to basal pyruvate-driven respiration by complemented $\Delta Mpc1$ cell lines as compared to WT+EV (N=12; 2 clone lines/genotype x 6 technical replicates/clone line).

D) Respiration driven by 1.0 mM pyruvate in cells described in **A**). 0.33 μ M FCCP was injected when indicated. Letters indicate significant difference in basal respiration among $\Delta Mpc1+EV$ (**a**; $P \leq 0.05$) versus WT+EV, in FCCP-stimulated respiration among $\Delta Mpc1+EV$, $\Delta Mpc1+L79H$, $\Delta Mpc1+A58G$ (**b-d**; $P \leq 0.001$) versus WT+EV, and in UK5099-inhibited respiration among $\Delta Mpc1+A58G$ (**e**; $P \leq 0.001$), $\Delta Mpc1+EV$ (**f**; $P \leq 0.05$) versus WT+EV (N=12; 2 clone lines/genotype x 6 technical replicates/clone line).

E) Quantification of FCCP-stimulated normalized to basal pyruvate-driven respiration by complemented $\Delta Mpc1$ cell lines as compared to WT+EV (N=12; 2 clone lines/genotype x 6 technical replicates/clone line).

F) Respiration driven by 1.0 mM pyruvate in cells described in **A**). 1.0 μ M FCCP was injected when indicated. Letters indicate significant difference in FCCP-stimulated respiration among $\Delta Mpc1+EV$, $\Delta Mpc1+WT$, $\Delta Mpc1+L79H$, $\Delta Mpc1+A58G$ (**a-d**; $P \leq 0.001$) versus WT+EV, and in UK5099-inhibited respiration among $\Delta Mpc1+EV$, $\Delta Mpc1+L79H$, $\Delta Mpc1+A58G$ (**e-g**; $P \leq 0.001$) versus WT+EV (N=4; 1 clone line/genotype x 4 technical replicates/clone line).

G) Quantification of FCCP-stimulated normalized to basal pyruvate-driven respiration by complemented $\Delta Mpc1$ cell lines as compared to WT+EV (N=4; 1 clone line/genotype x 4 technical replicates/clone line).

Data are presented as mean \pm SEM. One-way ANOVA was performed for Figure S5A-S5G (# # $p \leq 0.01$, # # # $p \leq 0.001$).

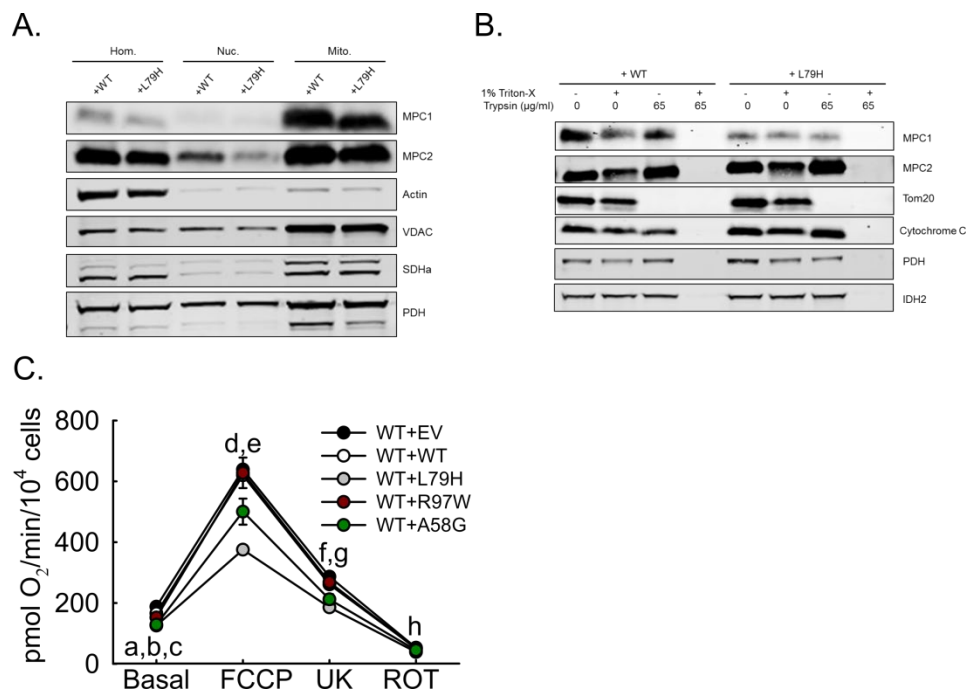


Figure S6. MPC1-L79H is trafficked to the mitochondria and accumulates in the inner membrane.

A) Representative MPC1, MPC2, Actin, VDAC, SDHa, and PDH levels visualized by immunoblot following fractionation of crude homogenate (Hom.) into nuclear (Nuc.) and mitochondrial (Mito.) fractions (N=4).

B) Representative MPC1, MPC2, Tom20, Cytochrome C, PDH, and IDH2 levels visualized by immunoblot following trypsin digestion in intact and disrupted isolated mitochondria from $\Delta Mpc1$ cells complemented with an empty vector (EV), plus WT human MPC1-FLAG ($\Delta Mpc1$ +MPC1-FLAG), or the MPC1-L79H-FLAG ($\Delta Mpc1$ +MPC1-L79H-FLAG) (N=4).

C) Respiration driven by 10 mM pyruvate in WT C2C12 cells complemented with an empty vector (EV), or WT human MPC1 (WT), or the MPC1 mutants (L79H, R97W, and A58G). Letters indicate significant difference in basal respiration among WT+L79H (**a**; $P \leq 0.001$), WT+A58G (**b**; $P \leq 0.01$), WT+A58G (**c**; $P \leq 0.05$) versus WT+EV, in FCCP-stimulated respiration among WT+L79H (**d**; $P \leq 0.001$), WT+A58G (**e**; $P \leq 0.01$) versus WT+EV, in UK5099-inhibited respiration among WT+L79H (**f**; $P \leq 0.001$), WT+A58G (**g**; $P \leq 0.01$) versus WT+EV, and in rotenone-inhibited respiration between WT+L79H (**h**; $P \leq 0.01$) versus WT+EV (N=12; 2 clone lines/genotype x 6 technical replicates/clone line).

Data are presented as mean \pm SEM. One-way ANOVA was performed for Figure S6C.

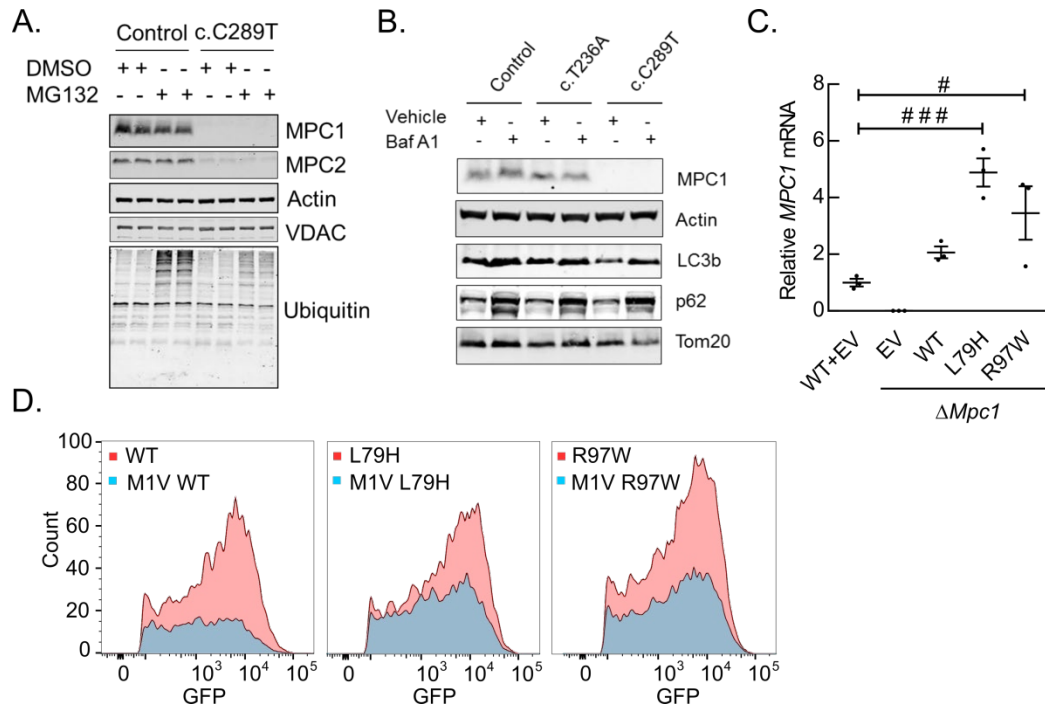


Figure S7. MPC1-R97W mRNA is stable, but protein is degraded by non-proteosomal and autophagy programs.

A) Representative MPC1, MPC2, Actin, VDAC, and Ubiquitinated protein levels visualized by immunoblot in immortalized wild-type (WT) and patient fibroblasts from Family 1 (c.C289T) following treatment with DMSO or the proteasome inhibitor MG132 (N=3).

B) Representative MPC1, Actin, VDAC, LC3b, p62, Tom20, PDH, and SDHa levels visualized by immunoblot in immortalized wild-type (WT) and patient fibroblasts from Family 3 (c.T236A) and Family 1 (c.C289T) following treatment with Vehicle or the autophagy inhibitor Bafilomycin a (N=4).

C) Quantification of *Mpc1* transcript in WT C2C12 cells transduced with a vector expressing guideless Cas9 and subsequently with an empty vector (WT+EV) or *MPC1* transcript in $\Delta Mpc1$ cells complemented with an empty vector (EV), plus WT human MPC1 (WT), or the MPC1 mutants (L79H and R97W). Statistics versus WT+EV (N=3).

D) Representative histogram of GFP fluorescence intensity assessed by flow cytometry in WT C2C12 cells were complemented with MPC1-P2A-GFP (WT) or M1V-MPC1-P2A-GFP (M1V WT), MPC1(L79H)-P2A-GFP (L79H) or M1V-MPC1(L79H)-P2A-GFP (M1V L79H), MPC1(R97W)-P2A-GFP (R97W) or M1V-MPC(R97W)-P2A-GFP (M1V R97W) (N=3).

Data are presented as mean \pm SEM. One-way ANOVA was performed for Figure S7C (# $p \leq 0.05$, ### $p \leq 0.001$).

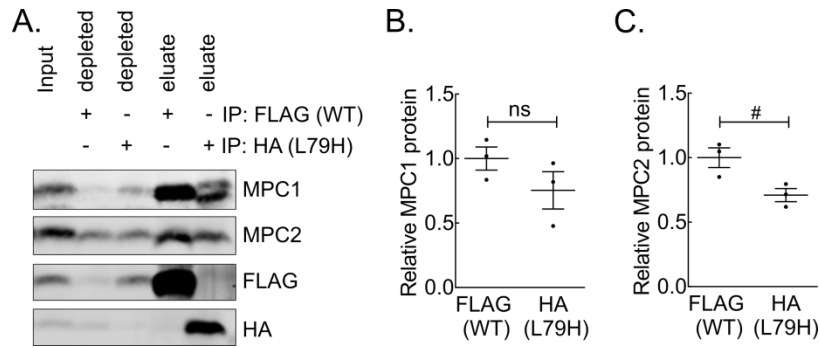


Figure S8 The MPC1(L79H)-MPC2 interaction is weaker than MPC1(WT)-MPC2, inverted –HA and –Flag tags.

A) Representative MPC1, MPC2, FLAG, and HA levels visualized by immunoblot in input, immune-depleted (depleted), wash, and eluate fractions from co-immunoprecipitation of MPC1 proteins (WT-FLAG or L79H-HA) precipitated using FLAG or HA antibodies in the $\Delta Mpc1$ cell line expressing both WT-FLAG and L79H-HA (N=3).

B-C) Quantification of relative MPC1 (B) and MPC2 (C) protein levels in eluates from the WT-FLAG and L79H-HA pull-down (N=3).

Data are presented as mean \pm SEM. Two-tailed unpaired t-test was performed for Figure S8B-S8C (# $p \leq 0.05$, ns=not significant).